Mathematical and Physical Modeling of Systems for Metal Delivery in the Continuous Casting of Steel and DC Casting of Aluminum

D. Xu[1], W.K. Jones, Jr.[1], J.W. Evans[1] and D.P. Cook[2]

1. Dept. of Materials Science and Mineral Engineering, University of California, Berkeley, CA USA
2. Reynolds Metals Company, Richmond, VA USA

ABSTRACT

In the continuous casting of steel, various nozzles have been used (e.g., bifurcated nozzles with ports inclined at various angles to the horizontal) to deliver metal from the tundish into the caster. An even greater variety of devices is used in the case of semi-continuous (DC or electromagnetic) casting of aluminum, for example, nozzles delivering metal into bags of various designs. The paper describes a physical (water) model whereby particle image velocimetry has been used to measure velocities. These measured velocities are compared to ones predicted using computational fluid dynamics. Conclusions are reached concerning the validity of the computations and recommendations made about improvement in casting operations by modification of melt flow.

1. INTRODUCTION AND OBJECTIVES

It has long been recognized that the micro-structure of a solidified metal can be affected by flow of the liquid metal during solidification (Sahm, 1982; Glicksman et al., 1986). For example, it is known that "fragmentation" of growing dendrite arms, together with the convection of the fragments to other regions of the melt, can provide nuclei initiating solidification in those regions (Paradies et al., 1991 and 1994). In the casting of real metals (as opposed to model organic solids), one's ability to observe and measure such convection are severely limited by the opacity of the melt and the high temperatures involved. Consequently there has been much simulation of flow in casting operations by both mathematical and physical modeling (Li and Anyalebechi, 1995, Grün et al., 1994, Thomas et al., 1994, Harris and Young, 1982, DeSanties and Ferretti, 1996, Flint, 1990, Thomas et al., 1990).

The present paper is a report of an on-going investigation into the flow within the liquid pool of casters used in the semi-continuous casting of aluminum; some preliminary results are also included on flow in steel casters. Aluminum is cast into ingots for subsequent rolling operations by either "Direct Chill" (DC) or electromagnetic (EM) casting. In either case the metal flows into the liquid pool at the top of the caster via a nozzle and a distributor bag. The nozzles are of various designs, as are the distributor bags; the latter serve to dissipate the momentum of the downward entering jet of aluminum and to distribute the hot metal, particularly toward the short sides of the ingot where cooling is usually greater. In steel casters the metal typically flows into the liquid pool through a submerged entry nozzle with two ports at its lower end. There are no distributor bags and the direction of the inflowing metal towards the short sides of the slab is achieved by these two ports. The metal inflow may be directed downward by a downward inclination of the axis of each port. The flow may be further affected by the common practice of injecting argon into the nozzle (so as to minimize air ingress and nozzle blockage by oxidation products) and also by the application of electromagnetic braking.There are other significant differences between the casting of aluminum and steel. Obvious ones are the temperatures involved and the oscillation of the mold in the latter case.

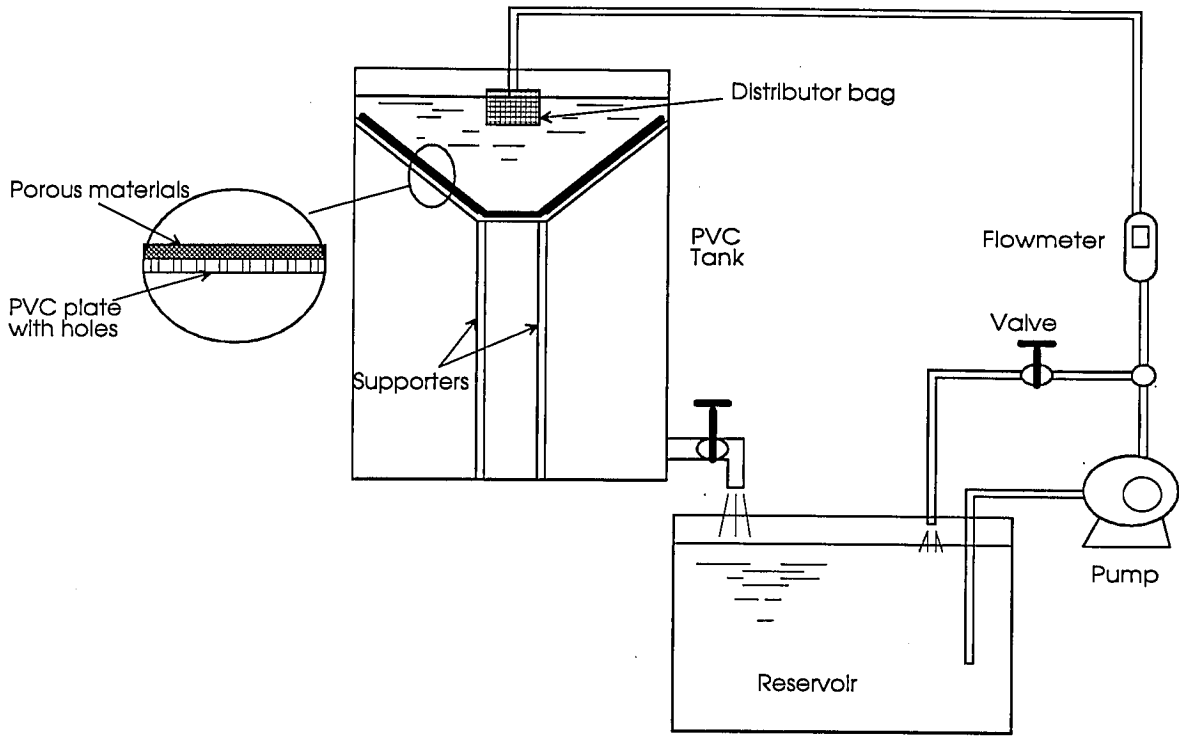

Figure 1. Sketch of the physical model

Another important difference is the casting speed which is of the order of 1mm/s for aluminum, but more than an order of magnitude greater for steel. Consequently the depth of the liquidpool ("sump") in aluminum casting is in the range of 0.3-0.5 m but approximately 2-4 m for steel, making the shapes of the sumps greatly different. The present investigation entails both an experimental and computational component. Experiments have been on a water model which can be used to simulate casting of either aluminum or steel. A difference between this modeling and much previous water modeling (particularly of steel casters) has been the quantitative determination of velocities by particle image velocimetry (PIV) (Adrian, 1986, Keane and Adrian, 1993). The mathematical modeling is being carried out using FIDAP. The ultimate objective of the investigation is to discover how metal inflow can be engineered so as to improve ingot characteristics (segregation, grain size etc.). The first step in this effort is to determine what flow fields result from the various equipment in use for controlling metal inflow.

2. EXPERIMENTAL INVESTIGATION

The apparatus is sketched (in the configuration simulating aluminum casting) in Fig 1. It consists of the model proper and a system for delivering water from a reservoir, through a pump and flowmeter to the model, from whence the water flows back to the reservoir. The model is a tank of clear PVC containing a nozzle, distributor bag and simulated solidification front.

In the real caster the liquid metal flows downward into the solidification front at a speed which is everywhere equal to the casting speed. That behavior is simulated for aluminum casting by positioning a sump-shaped construction of perforated PVC covered by a plastic material of relatively fine pores. In the case of steel casting simulations, this construction was removed and the water flowed under a baffle at the bottom of the tank before

exiting to the reservoir. The absence of a simulated solidification front is justified by the relatively small shell thickness in the mold region of actual casters. The results reported here for aluminum are early ones where the model was configured to be a half-model of a pilot scale caster producing ingots of 0.76 m by 0.3 m cross section. That is, the symmetry about a vertical plane passing through the nozzle and perpendicular to the long sides (rolling faces) of the ingot was exploited and this plane was developed using the wall of the tank with a half-nozzle placed against it. Such a simulation is imperfect in that the boundary condition at this surface (no slip) is different from that (free slip) in the real caster. Subsequently it was found that the flow is better represented by a full model and the results given below for steel are for a full model. Measurements of velocity in the model were carried out using PIV. This technique would normally require the use of a high power laser (>10W) to provide the necessary sheet illumination of the model. Such lasers are expensive and dangerous; a satisfactory alternative was 4.5kW of halogen lighting contained within an air-cooled box. Light from the box, highly collimated by a slit in the base, passed downward through the model as a sheet a few mm thick. Latex particles (150-200 micrometers), of near neutral density, were introduced into the flow from a dispenser connected to the nozzle. Those illuminated by a light sheet were imaged by a CCD camera connected to a computer. The frame-to-frame movement of particle images was analyzed by PIV software (Optical Flow Systems, Edinburgh) to produce vector plots of velocities over the interval (typically 33 milliseconds) between frames. Because the flow was turbulent, such vector plots varied with time and did not contain results that could be directly compared with computed time-averaged velocities, such as those produced by FIDAP. Consequently a large number of these plots were acquired at random times and averaged to yield an ensemble averaged vector plot that, it is assumed, approximated a time-averaged velocity. It was found that the ensemble average was essentially invariant after averaging 50 "instantaneous" vector plots. Fig 2 shows an instantaneous plot and is for a case where no distributor bag is used. These measurements are for a vertical plane parallel to the short side of the ingot and positioned 32 mm from the wall of the tank that simulates the symmetry plane (and therefore a little behind the nozzle). The V of the simulated solidification front is seen and the asymmetry of this instantaneous flow is apparent. The water flowrate was set to give a water velocity at the solidification front of 0.53 mm/s simulating a casting speed of 1.0 mm/s when Reynolds numbers are equated. This water velocity through the solidification front is small compared to the recirculation velocities of Fig. 2.

The time-averaged velocity map, synthesized from 50 plots similar to Fig. 2, appears as Fig. 3. To a good approximation the flow pattern is now seen to be symmetric, as expected. In both Figs. 2 and 3 the strong downward jet leaving the nozzle is apparent. This jet intersects the plane of measurement at approximately mid-height. Fig. 4 is the time-averaged velocity map for similar conditions, except that now a (half) distributor bag is placed between the nozzle and solidification front. The bag (a 'combo bag' in the terminology of the industry) directs the inflowing metal in a horizontal direction perpendicular to the page. Consequently, all that is visible in the plane of measurement is the weak recirculation, beneath the bag, induced by the inflow. Fig. 5 is the time-averaged vector plot for the water model used to simulate steel casting. One half of the upper region of the tank is illustrated; although, in this case, a full model is used (simulating a slab 1.52 m by 0.3 m in cross section), the flow is symmetric and only the left half is shown. The water enters through a nozzle with two ports (25.4 mm in diameter) and the ports (one close to the upper right of Fig. 5) are at a submergence of 170 mm with horizontal axes. The plane of Fig. 5 is the plane of these axes and the nozzle centerline. The strong outward jet from the port induces recirculation, both above and below the level of the port, the former being particularly rapid.

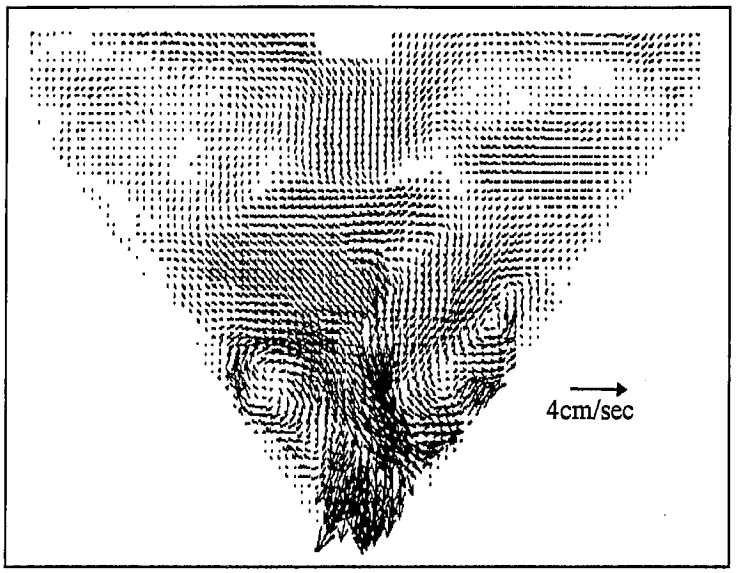

Figure 2. Instantaneous vector map

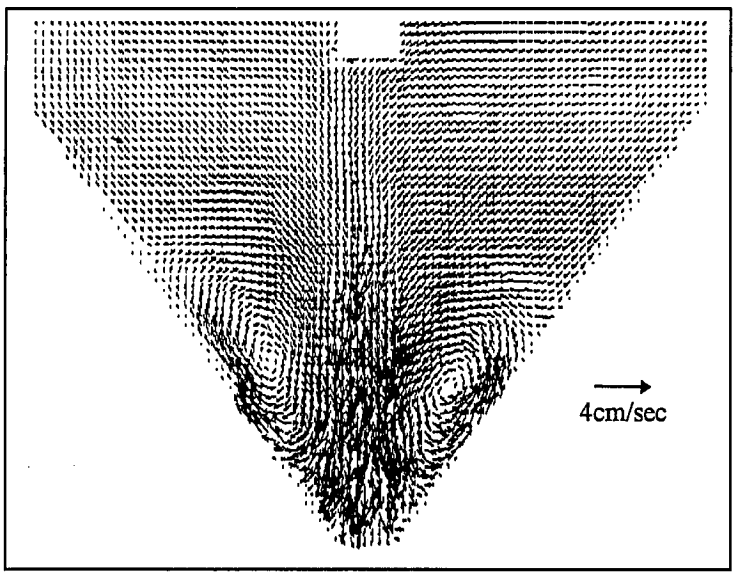

Figure 3. Time-averaged-vector (TAV) map

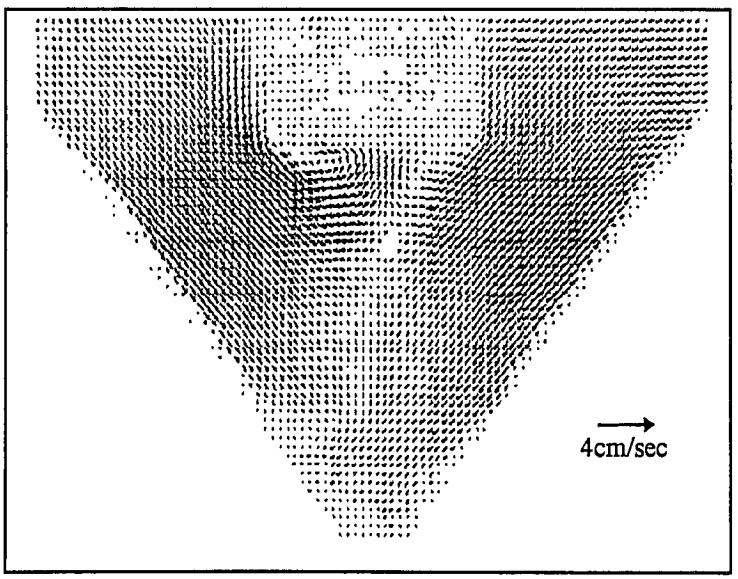

Figure 4. TAV map with bag

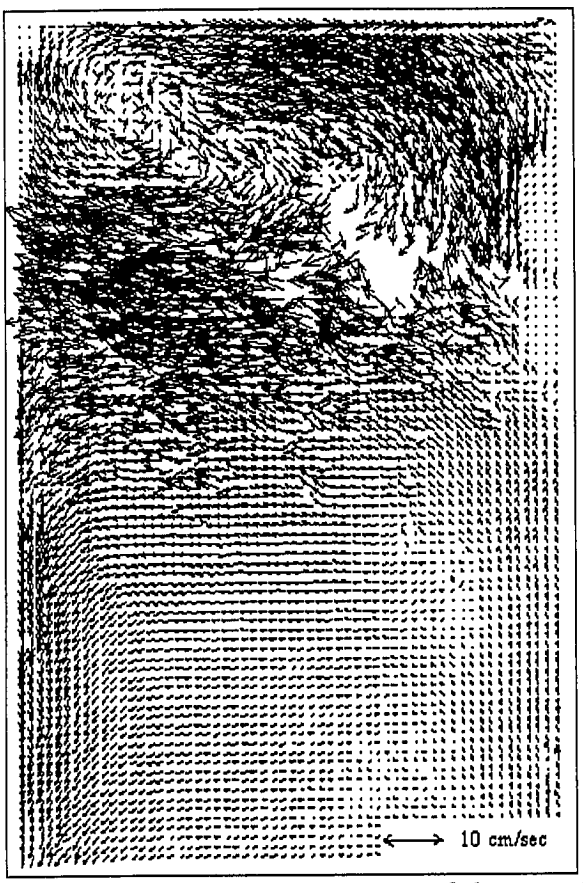

Figure 5. The TAV vector map of the central section through a 0° nozzle

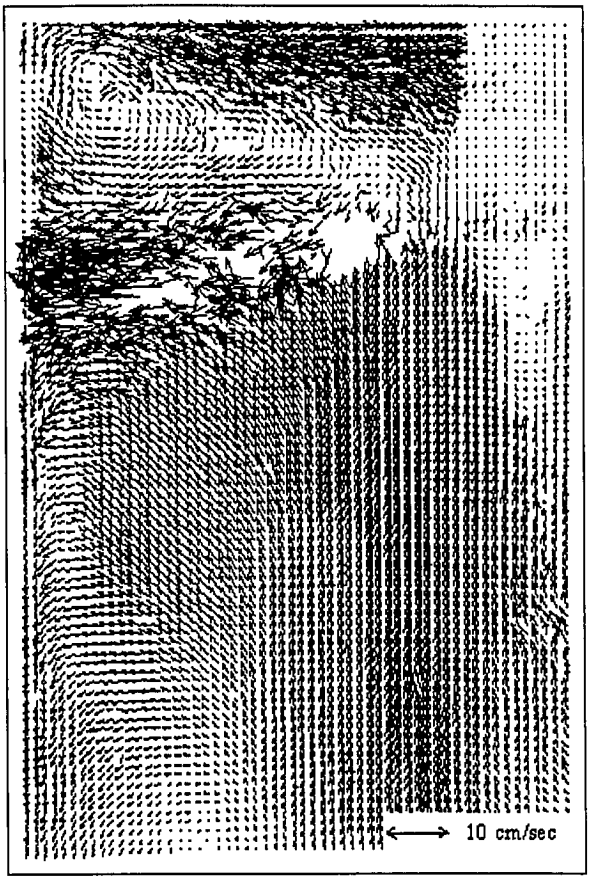

Figure 6. The TAV vector map of the central section through a 15° nozzle

With the ports angled downward by 15° (Fig. 6) the upper recirculation loop is less strong while the lower loop becomes stronger. The trend continues for the case where the ports are angled downward through 30°, as can be seen in Fig. 7. These three results are ones where no argon is injected and argon injection is likely to modify the flow significantly (e.g., by inducing a strong upflow in the region near the nozzle). The physical model also neglects the effects of thermal buoyancy and electromagnetic braking (if applied). There is insufficient space here to present additional results that have been obtained (e.g., the effect of twisting the inlet nozzle by a few degrees about its vertical axis).

3. COMPUTED VELOCITY FIELDS

The finite element software FIDAP was used to compute the time-averaged velocities in the physical models. In the case of the (simulated) aluminum caster the computations were three dimensional and the boundary conditions imposed were those seen in Fig. 8. [FIDAP imposes a zero gradient condition where the dependent variable is not specified on a boundary.] These boundary conditions were intended to match those of the half model used in the experiments, rather than the actual caster. Cases with and without a distributor bag were modeled. With the bag, the velocities at the bag were set equal to zero, except for the windows through which the water flowed. At these windows (or at the nozzle when the bag was absent) the velocity was adjusted by FIDAP to satisfy continuity, given the outflow through the solidification front. Calculations were performed using a segregated solution algorithm that required between 109 and 127 iterations, depending on the case, to reach convergence. Typically, 4800 4-node quadrilaterals and 16,800

Figure 7. The TAV vector map of the central section through a 30° nozzle

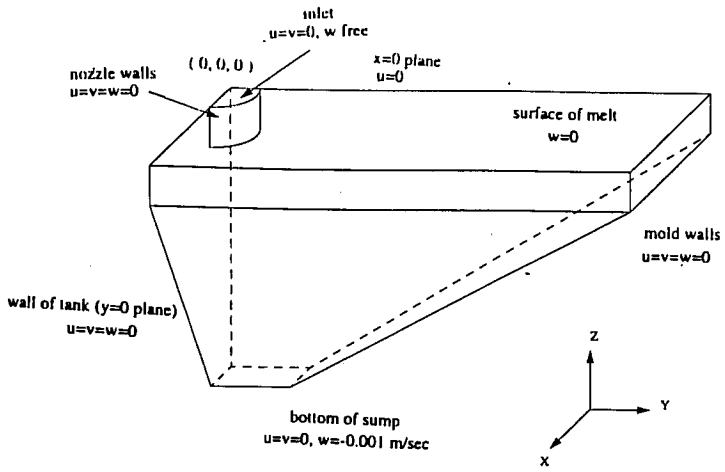

Figure 8. The boundary conditions imposed on the mathematical model

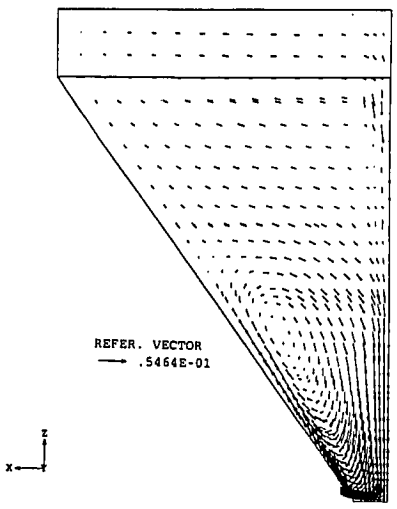

Figure 9. The calculated result for the case without a bag

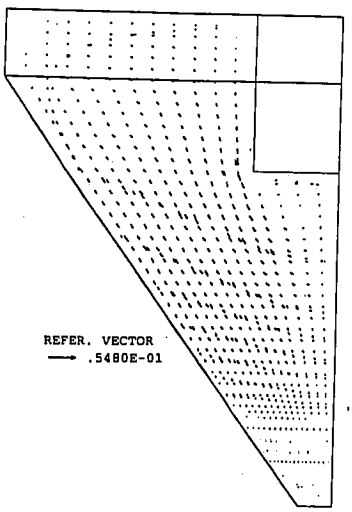

Figure 10. The calculated result for the case with a bag

8-node brick elements were used for the 2-D and 3-D simulations, respectively. Grid refinement was used in regions of large velocity gradients, i.e., near the nozzle and impingement wall. Due to the robust nature of the segregated solution, convergence was achieved in the 2-D cases within 45 minutes, while for the 3-D simulation it took several hours. Computations were run on both IBM RS6000 and Sun Sparc20 workstations. Computed results for the case of no distributor bag appear in Fig. 9 while Fig. 10 shows velocities computed for a bag present. The computed velocities are in qualitative agreement with the measurements of Figs. 3 and 4. In both experimental measurements and calculated velocities there is a strong downward jet in the center of the V of the solidification front with the bag absent, but only a relatively weak recirculating flow when the bag is in position.

As of the time of writing, only two-dimensional calculations have been carried out for the steel casting case. The water is considered to be entering the 2-D computational domain at the same speed as in the water model. The water then leaves the bottom of the domain at a speed sufficient to satisfy continuity. Because the jet from the nozzle port is precluded from spreading in the third dimension in the 2-D mathematical model, only approximate agreement can be expected between measurements and calculations. In particular the computed speed of the outflow will exceed the casting speed of the water model and velocities elsewhere, particularly away from the nozzle will be over-estimated. These expectations are realized in Figs. 11 and 12 for horizontal nozzle ports and ones inclined 15° downward, respectively. Fig 11 shows recirculation loops above and below the entry port, as in the measurements of Fig. 5. However the computed loops are comparable in speed while the measured ones show a stronger upper loop. The 2-D calculations over-estimate the upward velocities on the centerline below the nozzle by an order of magnitude.

The 2-D model also gives only qualitative agreement with the measurements, comparing Figs. 7 and 12. The point of impingement of the jet with the wall at the left

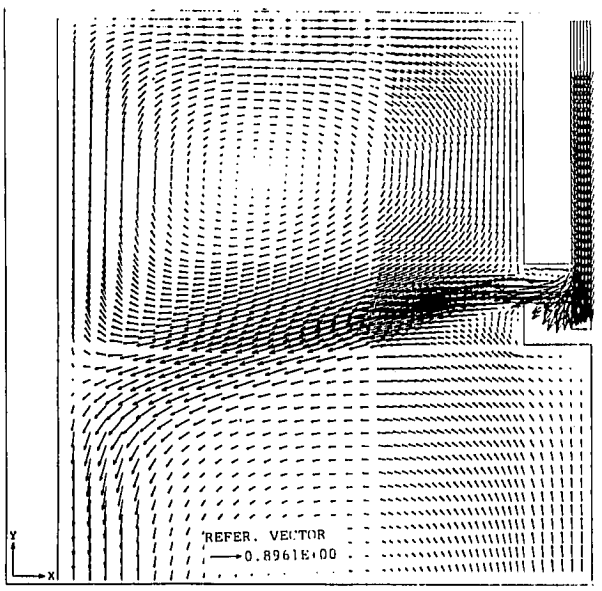

Figure 11. The calculated result for a 0° nozzle

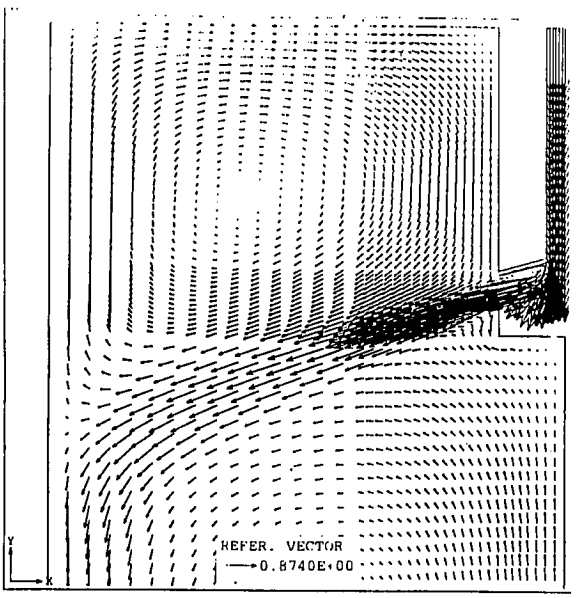

Figure 12. The calculated result for a 15° nozzle

side of the caster is approximately captured but the recirculation velocities below the nozzle are much higher in the computations than in the measurements.

4. CONCLUDING REMARKS

This paper has described physical and mathematical modeling that is in progress to determine how metal inflow systems for steel and aluminum casters can be engineered to improve the cast metal. The physical modeling differs from that of most previous measurements in that velocities have been measured by PIV. The measurements reveal a strong influence of the nozzle/distributor design on the flow pattern and velocities. Calculations of velocities using FIDAP have, to date, been only partially successful in reproducing the measured velocities.

ACKNOWLEDGMENTS

The authors are grateful to Reynolds Metals Company for financial support and for permission to publish these results.

REFERENCES

Sahm, P.R., 1982, The Role of Convection in Solidification", *Convective Heat Transport and Instability Phenomena.*, ed. Zierep, J. and Oertel Jr., H., pp. 515-556.

Glicksman, M.E., Coriell, S.R. and McFadden, G.B., 1986, Interaction of Flow with the Crystal-Melt Interface, *Ann. Rev. Fluid. Mech.*, **18**, pp. 307-335.

Paradies, C.J., Palmer, M.A. and Glicksman, M.E., 1991, Effects of Forced Flow on Remelting and Fragmentation of a Mushy Zone, *Light Metals*, pp. 863-867.

Paradies, C.J., Smith, R.N. and Glicksman, M.E., 1994, Effects of Mixed Convection on Dendrite Fragmentation During Alloy Solidification, *HTD-Vol. 284, Transport Phenomena in Solidification, ASME*, pp. 161-169.

Li, B.Q. and Anyalebechi, P.N., 1995, A Micro/macro Model for Fluid Flow Evolution and Microstructure Formation in Solidification Processes, *Int. J. Heat Mass Transfer*, **38**, pp. 2367-2381.

Grün, G.U., Eick, I. and Vogelsang, D., 1994, 3D-modeling of Fluid Flow and Heat Transfer for DC Casting of Rolling Ingots, *Light Metals*, pp. 863-868.

Thomas, B.G., Huang, X. and Sussman, R.C., 1994, Simulation of Argon Gas Flow Effects in a Continuous Slab Caster", *Metall. Trans. B*, **25**, pp. 527-547.

Harris, D.J. and Young, J.D., 1982, Water Modeling - a Viable Production Tool, *Steel-making Conf. Proc.*, **65**, pp. 3-16.

DeSanties, M. and Ferretti, A., 1996, Thermo-fluid-dynamics Modeling of the Solidification Process and Behavior of Non-metallic Inclusions in the Continuous Casting Slab", *ISIJ International*, **36**, pp. 681-689.

Flint, P.J., 1990, A Three-Dimensional Finite Difference Model of Heat Transfer, Fluid Flow and Solidification in the Continuous Slab Caster, *Steelmaking Conf. Proc.*, **73**, pp. 481-490.

Thomas, B.G., Mika, L.J. and Najjat, F.M., 1990, Simulation of Fluid Flow Inside a Continuous Slab-Casting Machine, *Metall. Trans. B*, **21**, pp. 387-400.

Adrian, R.J., 1986, Multi-Point Optical Measurement of Simultaneous Vectors in Unsteady Flow - a Review, *Int. J. Heat and Fluid Flow*, **7(2)**, pp. 127-145.

Keane, R.D. and Adrian, R.J., 1993, Theory of Cross-Correlation Analysis of PIV Images, *Flow Visualization and Image Analysis*, ed. Nieuwstadt, F.T.M, pp. 1-25.